

Summary Report
STUDY TO DOCUMENT
LOW THRUST TRAJECTORY OPTIMIZATION PROGRAMS
HILTOP AND ASTOP

(NASA-CR-120767) STUDY TO DOCUMENT LOW THRUST TRAJECTORY OPTIMIZATION PROGRAMS HILTOP AND ASTOP (Analytical Mechanics Associates, Inc.) CSCL 22C 63/13 N75-23635 Unclas 21907

Jerry L. Horsewood
Frederick I. Mann
Samuel Pines

PRICES SUBJECT TO CHANGE

AMA, Inc. Report No. 74-32
Contract NAS8-29945
December 1974

Reproduced by
NATIONAL TECHNICAL
INFORMATION SERVICE
U.S. Department of Commerce
Springfield, VA. 22151

ANALYTICAL MECHANICS ASSOCIATES, INC.
10210 GREENBELT ROAD
SEABROOK, MARYLAND 20801

ABSTRACT

This report describes the work carried out under Contract NAS8-29945, "Conversion of HILTOP and ASTOP Computer Programs." The study entailed the detailed documentation of the programs, the delivery of IBM 360 versions of the programs to the NASA Marshall Space Flight Center, and the investigation of selected topics relating to the possible extension of the HILTOP program. The documentation of the computer programs is being published concurrently with this summary report, and the programs have been delivered. This report presents the analyses of the possible HILTOP extension and also gives the results of an extra-ecliptic mission study performed with HILTOP.

PRECEDING PAGE BLANK NOT FILMED

TABLE OF CONTENTS

	page
ABSTRACT	iii
I. INTRODUCTION AND SUMMARY	1
II. GENERALIZED ANALYSIS OF FIXED THRUST CONE ANGLES	5
III. GENERALIZED RANK-PRESERVING SEARCH ALGORITHM	15
IV. TRAJECTORY OPTIMIZATION CONSIDERING THRUSTER THROTTLING	21
V. INFINITESIMAL THRUST/COAST PHASES	27
VI. CURSORY TRAJECTORY ANALYSIS OF THE EXTRA- ECLIPTIC MISSION	31
VII. REFERENCES	37

PRECEDING PAGE BLANK NOT FILMED

I. INTRODUCTION AND SUMMARY

The primary purpose of this study was to develop detailed documentation for two existing low thrust trajectory optimization computer programs: (1) HILTOP, a variational calculus program for optimizing heliocentric trajectories in a central force gravitational field; and (2) ASTOP, a parameter optimization program for n-body interplanetary trajectories.

Prior to documenting HILTOP, a concerted effort was undertaken to reduce the core requirements of the program to facilitate its use at installations where core availability is at a premium. This reduction in program size was achieved through various techniques, such as reduction of array dimensions and elimination of selected subroutines. None of the modifications made restrict or degrade the program's capabilities, although a small degradation in efficiency will result for some mission types. For example, separate routines to handle two-dimensional missions were removed. The core requirements were reduced about 25 percent. The documentation ^[1] is being published concurrently with this summary report.

Much more extensive changes were made to ASTOP before and during documentation. Unlike HILTOP, ASTOP is a research program which had been used very little and contained much unused code that remained from the ITEM program from which ASTOP was derived. The first step undertaken was to pass the source code through various utility programs which reordered the non-executable statements (such as type statements, dimensions, commons, data and equivalence statements), sequenced the statement numbers and, in general, cleaned-up the code. This was followed by passing the new source code through additional utility programs which generated various cross reference tables of subroutines, labelled commons and common variables. A careful scrutiny of the compilation listings in conjunction with these cross reference tables resulted in the elimination of certain subroutines, commons, blocks of code and selected variables from the program because they were not used. The program was then debugged and forced to execute a test case to assure that no serious oversights had occurred. The entire process was then

repeated, again resulting in a significant reduction in non-productive code, and the documentation of subroutines was then begun. During the documentation process, virtually every line of code was studied and several additional changes were effected. In all, the region size was reduced from about 480 K to 336 K. The documentation for ASTOP is given in Reference [2].

The study also called for the investigation of several potential extensions to the HILTOP program. These were:

- (1) extension of fixed thrust cone angle logic to include multiple cone angles;
- (2) generalization of fixed thrust cone angle logic to permit solar array orientation to be non-normal to the sun line;
- (3) improve the convergence characteristics of the iterator;
- (4) include solar array radiation degradation effects in the performance and optimization model;
- (5) generalize the propulsion system model to include variable specific impulse and efficiency as a function of throttling ratio; and
- (6) alleviate convergence problems manifested by infinitesimal thrust or coast phases.

None of the above extensions was implemented in HILTOP as part of this study because the magnitude of the task exceeded the funds available. Each potential extension was studied, although at varying levels of detail.

The items (1) and (2) above were formulated within the same general problem, and the detailed analysis is presented in Section II. With regard to item (3), a new iterator was developed; however, the approach was designed to speed the computations on each iteration rather than improve the convergence rate. A detailed discussion of this iterator is given in Section III. A radiation degradation model was actually implemented in HILTOP as part of a separate study. The intent of item (4) was to improve this model using inputs to be provided through MSFC. Since no revised model was developed, no further analysis was undertaken. A detailed

description of the current model is given in [1]. A model of thruster throttling effects was incorporated in an early version of HILTOP but, because its use was rather expensive, this model was not included in the current version. An analysis of the principal requirements of such a feature is presented in Section IV. The convergence problems alluded to in item (6) have been given considerable thought and, as yet, no satisfactory solution has been found. The present understanding of the problems is discussed in Section V.

During the course of the study, an analysis was performed of extra-ecliptic missions using the SEP stage atop a Titan III E/Centaur launch vehicle. Several trajectory classes involving mission durations from $1\frac{1}{2}$ to 3 years were investigated for heliocentric inclinations ranging from 45 to 60 degrees. The results of this analysis are presented in Section VI.

II. GENERALIZED ANALYSIS OF FIXED THRUST CONE ANGLES

Optimal trajectories with unconstrained thrust direction will frequently result in a thrust angle relative to the sun line that fluctuates over a wide range during the course of the trajectory. With SEP systems, for which the arrays are usually assumed to continuously face the sun, this requires a continual movement of the thrusters relative to the arrays, a requirement that is highly undesirable. For this reason the concept of operating the system with a fixed spacecraft array configuration is of much interest. The capability of simulating this constraint has been available in HILTOP for some time. However, the performance penalty incurred in some missions with a single fixed cone angle is excessive, so the ability to define the performance sensitivity to a number of fixed angles is desired.

The following development represents an extension to the formulation of the HILTOP program as presented in Reference [1]. Familiarity with these two documents is essential to the clear understanding of the analysis which follows.

Consider the case of a solar electric spacecraft with solar array orientation defined by the unit vector \bar{n} and thrust in the direction of the unit vector \bar{e}_t , and suppose that \bar{e}_t is constrained to lie nominally at one of a number of specified cone angles ϕ_i , $i = 1, 2, \dots, k$, from \bar{n} . Also, to provide for the option of thrust vectoring, admit the possibility that \bar{e}_t may lie anywhere within a cone of specified half angle η_i about the nominal directions defined by ϕ_i . (See the sketches at the end of this section). This constraint may be expressed mathematically by the inequality

$$\psi_1 = (\cos^{-1} (\bar{e}_t \cdot \bar{n}) - \phi_i)^2 - \eta_i^2 \leq 0. \quad (2-1)$$

In addition, it may be desirable in certain cases to orient the solar arrays to continuously maintain maximum power output. This may be accomplished by imposing the constraint

$$\psi_2 = \bar{n} \cdot \bar{e}_r - 1 = 0 \quad \text{for } r \geq r_c,$$

or

$$\psi_2 = \bar{n} \cdot \bar{e}_r - r^2/r_c^2 = 0 \quad \text{for } r < r_c,$$

where $\bar{e}_r = R/r$ and r_c is a specified solar distance below which the arrays are tilted so as to maintain constant power output of the arrays for $r < r_c$.

To the state equations given in [1], we add for this problem the k equations

$$\dot{\phi}_i = 0, \quad i = 1, 2, \dots, k.$$

These are included to yield associated adjoint variables which will appear in transversality conditions if it is desired to optimize the k cone angles.

The variational Hamiltonian for this problem is written

$$\begin{aligned} h_v = h_\sigma & \left[\frac{g\gamma}{\nu} (\Lambda \cdot \bar{e}_t - \frac{\nu}{c} \lambda_\nu) + \lambda_\tau \right] - \frac{\mu}{r^3} (\Lambda \cdot R) - \dot{\Lambda} \cdot \dot{R} \\ & + \lambda_{x_i} \left[(\cos^{-1}(\bar{e}_t \cdot \bar{n}) - \phi_i)^2 - \eta_i^2 \right] + \lambda_y (\bar{n} \cdot \bar{e}_r - \rho), \end{aligned} \quad (2-2)$$

where $\rho = r^2/r_c^2$ if $r < r_c$ and $\rho = 1$ otherwise. Of course, λ_{x_i} and/or λ_y are zero if the associated constraints are not imposed. The optimal control problem now is to choose \bar{e}_t , \bar{n} , and h_σ at each point along the trajectory so as to maximize h_v subject to the specified constraints. Since the last two terms in (2-2) never contribute to the magnitude of h_v , it is seen by inspection that h_v is maximized with respect to \bar{e}_t and \bar{n} by choosing \bar{e}_t as close to Λ as possible and choosing \bar{n} so as to make γ as large as possible. Of course, any constraints between \bar{e}_t and \bar{n} preclude choosing \bar{e}_t and \bar{n} independently; therefore, it is, in general, necessary to compromise in maximizing γ and $(\bar{e}_t \cdot \Lambda)$ individually in favor of maximizing the function $\gamma(\Lambda \cdot \bar{e}_t - \frac{\nu}{c} \lambda_\nu)$. This must be done by considering individual cases that may arise.

First, consider the case for which the solar arrays orientation is constrained so as to produce maximum power output. Under this constraint one

can consider maximizing h_v only after the constraint is satisfied, and maximizing h_v is equivalent to maximizing $(\Lambda \cdot \bar{e}_t)$ subject to the constraint. Let α denote the angle between R and Λ and let j denote the index of the currently optimum cone angle (the determination of which cone angle is currently optimum will be considered subsequently). Then, for $r > r_c$, the constraint of maximum-power output requires that $\bar{n} = \bar{e}_r$, and the choice of \bar{e}_t which maximizes $(\Lambda \cdot \bar{e}_t)$, and therefore h_v , subject to the constraint is

$$\bar{e}_t = \begin{cases} \bar{e}_r \cos(\phi_j + \eta_j) + (\bar{m} \times \bar{e}_r) \sin(\phi_j + \eta_j) & \text{if } \alpha \geq \phi_j + \eta_j \\ \bar{e}_\lambda & \text{if } \phi_j - \eta_j < \alpha < \phi_j + \eta_j \\ \bar{e}_r \cos(\phi_j - \eta_j) + (\bar{m} \times \bar{e}_r) \sin(\phi_j - \eta_j) & \text{if } \alpha \leq \phi_j - \eta_j \end{cases}$$

where $\bar{e}_\lambda = \Lambda/\lambda$ and $\bar{m} = (R \times \Lambda)/|R \times \Lambda|$. For $r < r_c$, \bar{n} is constrained to lie on a cone of half-angle

$$\theta = \cos^{-1}(r^2/r_c^2),$$

about \bar{e}_r , and the optimal choice for \bar{e}_t is

$$\bar{e}_t = \begin{cases} \bar{e}_r \cos(\phi_j + \eta_j + \theta) + (\bar{m} \times \bar{e}_r) \sin(\phi_j + \eta_j + \theta) & \text{if } \alpha \geq \phi_j + \eta_j + \theta \\ \bar{e}_\lambda & \text{if } \phi_j - \eta_j - \theta < \alpha < \phi_j + \eta_j + \theta \\ \bar{e}_r \cos(\phi_j - \eta_j - \theta) + (\bar{m} \times \bar{e}_r) \sin(\phi_j - \eta_j - \theta) & \text{if } \alpha \leq \phi_j - \eta_j - \theta \end{cases} \quad (2-3)$$

while \bar{n} (which is not always unique) may be defined

$$\bar{n} = \begin{cases} \bar{e}_r \cos \theta + (\bar{m} \times \bar{e}_r) \sin \theta & \text{if } \alpha \geq \phi_j + \theta \\ \bar{e}_r \cos \theta + (\bar{m} \times \bar{e}_r) \sin \theta \cos \epsilon + \bar{m} \sin \theta \sin \epsilon & \text{if } \phi_j - \theta < \alpha < \phi_j + \theta \\ \bar{e}_r \cos \theta - (\bar{m} \times \bar{e}_r) \sin \theta & \text{if } \alpha \leq \phi_j - \theta \end{cases} \quad (2-4)$$

where $\epsilon = \cos^{-1} \left[(\cos \phi_j - \cos \theta \cos \alpha) / \sin \theta \sin \alpha \right]$. Note that equations (2-3) and (2-4) also hold for the case $r > r_c$ if one sets $\theta = 0$.

For the case in which \bar{n} is not constrained to continuously yield maximum power output of the arrays, the optimal control problem becomes one of maximizing the function $\gamma (\bar{e}_\lambda \cdot \bar{e}_t - b)$ subject to the cone angle inequality constraint (2-1), where $b = \lambda_\nu \nu / c\lambda$. As in the preceding case, when $\phi_j - \eta_j - \theta < \alpha < \phi_j + \eta_j + \theta$ the quantities γ and $\bar{e}_\lambda \cdot \bar{e}_t$ may be maximized independently while satisfying the cone angle constraint by rotating \bar{n} out of the plane of R and Λ . When α is not within this interval, both \bar{n} and \bar{e}_t must lie in the plane of R and Λ and the maximization of $\gamma (\bar{e}_\lambda \cdot \bar{e}_t - b)$ may be taken with respect to a single parameter, say the angle δ between \bar{e}_λ and \bar{e}_t . (See Figure 2 at the end of this section). This is accomplished by solving the equation

$$(\cos \delta - b) \frac{\partial \gamma}{\partial \delta} - \gamma \sin \delta = 0, \quad (2-5)$$

for δ subject to the condition

$$(\cos \delta - b) \frac{\partial^2 \gamma}{\partial \delta^2} - 2 \sin \delta \frac{\partial \gamma}{\partial \delta} - \gamma \cos \delta \leq 0,$$

to assure the function is maximized. The solution of the equation (2-5) for δ will, for most forms of γ , require an iterative technique. For our purposes, γ written in terms of δ is of the form

$$\gamma = \sum_{i=0}^4 a_i \left(\frac{\cos (\alpha - \phi_j - \eta_j - \delta)}{r^2} \right)^{((i+4)/4)},$$

so that

$$\frac{\partial \gamma}{\partial \delta} = \tan (\alpha - \phi_j - \eta_j - \delta) \sum_{i=0}^4 a_i \left(\frac{i+4}{4} \right) \left(\frac{\cos (\alpha - \phi_j - \eta_j - \delta)}{r^2} \right)^{((i+4)/4)}.$$

A suggested approach to the solution of equation (2-5) is to employ a Newton's iteration with $\sin \delta$ as the independent variable, using as a first guess

$$\sin \delta = \frac{1-b}{2-b} \tan (\alpha - \phi_j - \eta_j) .$$

Once the optimum value of $\sin \delta$ is obtained, form $\cos \delta = \sqrt{1 - \sin^2 \delta}$ and write

$$\bar{e}_t = \bar{e}_\lambda \cos \delta - (\bar{m} \times \bar{e}_\lambda) \sin \delta ,$$

$$\bar{n} = \bar{e}_t \cos (\phi_j + \eta_j) - (\bar{m} \times \bar{e}_t) \sin (\phi_j + \eta_j) \quad \text{if } \alpha > \phi_j + \eta_j + \theta$$

or
$$\bar{n} = \bar{e}_t \cos (\phi_j - \eta_j) - (\bar{m} \times \bar{e}_t) \sin (\phi_j - \eta_j) \quad \text{if } \alpha < \phi_j - \eta_j - \theta .$$

Of course, if $\phi_j - \eta_j - \theta < \alpha < \phi_j + \eta_j + \theta$, then

$$\bar{e}_t = \bar{e}_\lambda ,$$

$$\bar{n} = \bar{e}_r \cos \theta + (\bar{m} \times \bar{e}_r) \sin \theta \cos \epsilon + \bar{m} \sin \theta \sin \epsilon ,$$

with

$$\epsilon = \begin{cases} 0 & \text{if } \alpha \geq \phi_j + \theta \\ \cos^{-1} \left[(\cos \phi_j - \cos \theta \cos \alpha) / \sin \theta \sin \alpha \right] & \text{if } \phi_j - \theta < \alpha < \phi_j + \theta . \\ \pi & \text{if } \alpha \leq \phi_j - \theta \end{cases}$$

To determine which of the ϕ_i is optimum at any instant, assume that $\phi_1 < \phi_2 < \dots < \phi_k$, and suppose that, at this instant,

$$\phi_i + \eta_i + \theta < \alpha < \phi_{i+1} - \eta_{i+1} - \theta .$$

Then j , the index of the optimum cone angle at that instant is

$$j = \begin{cases} i & \text{if } (\phi_{i+1} - \eta_{i+1} - \alpha) - (\alpha - \phi_i - \eta_i) > 0 \\ i+1 & \text{if } (\phi_{i+1} - \eta_{i+1} - \alpha) - (\alpha - \phi_i - \eta_i) < 0 \end{cases} .$$

The switch from one cone angle to the other occurs when the difference vanishes.

Since h_ν is linear in h_σ , the choice of h_σ is made as described in [1].

The adjoint equations are obtained formally through partial differentiation of the variational Hamiltonian. Those that differ from the adjoint equations presented in [3] are

$$\ddot{\Lambda} = \frac{3\mu}{r^5} (\Lambda \cdot R) R - \frac{\mu}{r^3} \Lambda + \frac{1}{r} \left[h_\sigma \frac{g\gamma'}{\nu} (\Lambda \cdot \bar{e}_t - \frac{\nu}{c} \lambda_\nu) + h_\rho \lambda_y \right] \left[\bar{n} - 3(\bar{e}_r \cdot \bar{n}) \bar{e}_r \right]$$

$$\dot{\lambda}_{\phi_j} = 2\lambda_{x_j} \left[\cos^{-1}(\bar{e}_t \cdot \bar{n}) - \phi_j \right]; \quad \dot{\lambda}_{\phi_i} = 0 \quad \text{for } i \neq j,$$

where

$$\gamma' = \frac{1}{r^2} \sum_{i=0}^4 a_i \left(\frac{i+4}{4} \right) \left(\frac{\bar{e}_r \cdot \bar{n}}{r^2} \right)^{i/4},$$

and

$$h_\rho = \begin{cases} 0 & \text{if } r > r_c \\ 1 & \text{if } r < r_c \end{cases}.$$

The Lagrange multipliers λ_{x_i} and λ_y are determined by setting the variations in h_ν resulting from independent variations in \bar{e}_t and \bar{n} , respectively, to zero. That is,

$$\left[h_\sigma \frac{g\gamma'}{\nu} \Lambda - 2\lambda_{x_i} \frac{(\cos^{-1}(\bar{e}_t \cdot \bar{n}) - \phi_j)}{\sqrt{1 - (\bar{e}_t \cdot \bar{n})^2}} \bar{n} \right] \cdot \delta \bar{e}_t = 0, \quad (2-6)$$

$$\left\{ \left[h_\sigma \frac{g\gamma'}{\nu} (\Lambda \cdot \bar{e}_t - \frac{\nu}{c} \lambda_\nu) + \lambda_y \right] \bar{e}_r - 2\lambda_{x_i} \frac{(\cos^{-1}(\bar{e}_t \cdot \bar{n}) - \phi_j)}{\sqrt{1 - (\bar{e}_t \cdot \bar{n})^2}} \bar{e}_t \right\} \cdot \delta \bar{n} = 0. \quad (2-7)$$

Now, because the variation of a unit vector must be normal to the unit vector, it is clear that $\delta \bar{e}_t$ may be divided into two components - one along $(\bar{n} \times \bar{e}_t)$

and the other along $(\bar{\mathbf{n}} \times \bar{\mathbf{e}}_t) \times \bar{\mathbf{e}}_t$. Since variations in these two directions are independent, the equation containing $\delta \bar{\mathbf{e}}_t$ must be satisfied by the variation along each component independently. Substituting into (2-6) the variation along $\bar{\mathbf{n}} \times \bar{\mathbf{e}}_t$ and using the identity $\bar{\mathbf{n}} \cdot (\bar{\mathbf{n}} \times \bar{\mathbf{e}}_t) = 0$ leads to the result

$$\Lambda \cdot (\bar{\mathbf{n}} \times \bar{\mathbf{e}}_t) = 0,$$

which indicates that Λ , $\bar{\mathbf{n}}$ and $\bar{\mathbf{e}}_t$ are coplanar vectors. Then, substituting into (2-6) the variation along the second component yields the desired definition of λ_{x_i} . Employing the identities

$$\begin{aligned} \Lambda \cdot [(\bar{\mathbf{n}} \times \bar{\mathbf{e}}_t) \times \bar{\mathbf{e}}_t] &= -(\bar{\mathbf{n}} \times \bar{\mathbf{e}}_t) \cdot (\Lambda \times \bar{\mathbf{e}}_t), \\ \bar{\mathbf{n}} \cdot [(\bar{\mathbf{n}} \times \bar{\mathbf{e}}_t) \times \bar{\mathbf{e}}_t] &= -(\bar{\mathbf{n}} \times \bar{\mathbf{e}}_t) \cdot (\bar{\mathbf{n}} \times \bar{\mathbf{e}}_t) = -(1 - (\bar{\mathbf{e}}_t \cdot \bar{\mathbf{n}})^2), \\ \bar{\mathbf{m}} &= (\bar{\mathbf{n}} \times \bar{\mathbf{e}}_t) / |\bar{\mathbf{n}} \times \bar{\mathbf{e}}_t|, \end{aligned}$$

yields for λ_{x_i}

$$\lambda_{x_j} = h_\sigma \frac{g\gamma}{\nu} \frac{\bar{\mathbf{m}} \cdot (\Lambda \times \bar{\mathbf{e}}_t)}{2[\cos^{-1}(\bar{\mathbf{e}}_t \cdot \bar{\mathbf{n}}) - \phi_j]}; \quad \lambda_{x_i} = 0 \quad \text{for } i \neq j.$$

Note that the identity involving $\bar{\mathbf{m}}$ is valid only outside the interval

$$\phi_j - \eta_j - \theta < \alpha < \phi_j + \eta_j + \theta,$$

but, since $\Lambda \times \bar{\mathbf{e}}_t$ becomes the null vector when α is within the interval, the above expression for λ_{x_j} is valid for all α .

Before defining λ_y recall that λ_y is non-zero only if the array orientation is constrained to yield maximum power output. Also note that λ_y appears only in the equation for $\ddot{\Lambda}$ where it is multiplied by the step function h_ρ . Therefore, λ_y influences the problem only when the array orientation constraint is imposed and when $r < r_c$, and we will confine the discussion of λ_y to cases where those conditions apply. Proceeding as with $\delta \bar{\mathbf{e}}_t$, consider

$\delta \bar{n}$ broken down into the two components along $(\bar{n} \times \bar{e}_t)$ and $[(\bar{n} \times \bar{e}_t) \times \bar{n}]$. Employing in (2-7) first the component along $(\bar{n} \times \bar{e}_t)$ and noting the identity $\bar{e}_t \cdot (\bar{n} \times \bar{e}_t) = 0$, one is left with the condition

$$\left[h_{\sigma} \frac{g\gamma'}{\nu} (\Lambda \cdot \bar{e}_t - \frac{\nu}{c} \lambda_{\nu}) + \lambda_y \right] [\bar{e}_r \cdot (\bar{n} \times \bar{e}_t)] = 0 .$$

Now, when α is outside the interval

$$\phi_j - \eta_j - \theta < \alpha < \phi_j + \eta_j + \theta ,$$

\bar{e}_r , \bar{n} and \bar{e}_t are coplanar such that $\bar{e}_r \cdot (\bar{n} \times \bar{e}_t) = 0$, and no information is given about λ_y . However, when α is within the interval, \bar{n} is rotated out of the plane of R and \bar{e}_t , and λ_y is then defined by the relation

$$h_{\sigma} \frac{g\gamma'}{\nu} (\Lambda \cdot \bar{e}_t - \frac{\nu}{c} \lambda_{\nu}) + \lambda_y = 0 .$$

It remains to define λ_y when α is outside the interval, and this is done by considering the component of $\delta \bar{n}$ along $(\bar{n} \times \bar{e}_t) \times \bar{n}$. Employing the identities

$$\bar{e}_t \cdot [(\bar{n} \times \bar{e}_t) \times \bar{n}] = (\bar{n} \times \bar{e}_t) \cdot (\bar{n} \times \bar{e}_t) = 1 - (\bar{e}_t \cdot \bar{n})^2 ,$$

$$\bar{e}_r \cdot [(\bar{n} \times \bar{e}_t) \times \bar{n}] = (\bar{n} \times \bar{e}_t) \cdot (\bar{n} \times \bar{e}_r) ,$$

$$\bar{m} = (\bar{n} \times \bar{e}_t) / |\bar{n} \times \bar{e}_t| ,$$

and substituting in (2-7) for λ_{x_i} leads to the relation

$$h_{\sigma} \frac{g\gamma'}{\nu} (\Lambda \cdot \bar{e}_t - \frac{\nu}{c} \lambda_{\nu}) + \lambda_y = h_{\sigma} \frac{g\gamma'}{\nu} \frac{\bar{m} \cdot (\Lambda \times \bar{e}_t)}{\bar{m} \cdot (\bar{n} \times \bar{e}_r)} ,$$

which completes the possible cases for which it is necessary to define λ_y .

As a final point, it should be noted that the transversality conditions to be satisfied if the k fixed cone angles ϕ_i are to be optimized are, simply,

$$\lambda_{\phi_i}(t_f) - \lambda_{\phi_i}(t_0) = 0; \quad i = 1, 2, \dots, k$$

where, without loss of generality, $\lambda_{\phi_i}(t_0)$ may be set to zero.

In summary, it is helpful to note the principal modifications to HILTOP that are required to implement the generalized cone angle logic. These are:

(1) At the start of each thrust phase, determine the index j of the optimum cone angle as prescribed in the text above.

(2) At each point along the trajectory, monitor the function*

$$(\phi_j + \phi_{j-1}) - (\eta_j - \eta_{j-1}) - 2\alpha.$$

When the function becomes positive, it is necessary to iterate to the time that the function is zero. At that time, decrement j by one, re-evaluate all derivatives for the new cone angle and continue integrating.

(3) At each point along the trajectory, monitor the function*

$$(\phi_{j+1} + \phi_j) - (\eta_{j+1} - \eta_j) - 2\alpha.$$

When this function becomes negative, it is necessary to iterate to the time that the function goes to zero. At that time, increment j by one, re-evaluate all derivatives for the new cone angle and continue integrating.

(4) Add the new terms to the derivatives $\ddot{\Lambda}$.

(5) Add an additional equation to the integrator; i.e., that required for $\lambda_{\phi_j}^\circ$.

Note that only one additional equation need be integrated at any instant in time since $\lambda_{\phi_i}^\circ = 0$ for $i \neq j$.

(6) Add the additional transversality conditions, $\lambda_{\phi_i}(t_f) = 0$.

(7) Add the computation of λ_{x_i} and λ_y .

(8) For cases in which \bar{n} is not constrained to lie along \bar{e}_r , the iterative solution of Equation (2-5) is required at every derivative evaluation. This will

*During thrust phases only.

significantly increase the CPU time required to integrate a trajectory.

- (9) Evaluate the unit vectors \bar{e}_t and \bar{n} .

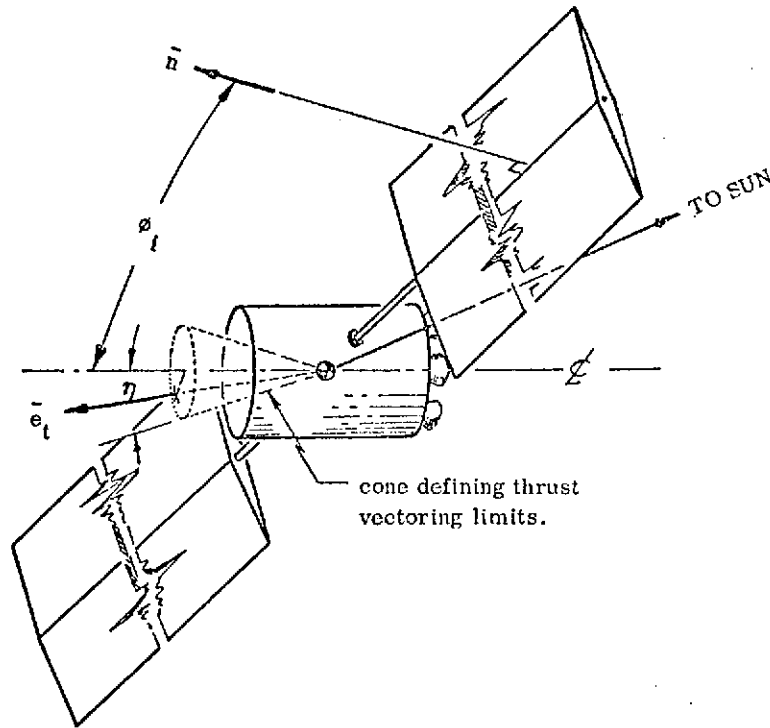


Fig. 1. Spacecraft geometry and nomenclature.

ORIGINAL PAGE IS
OF POOR QUALITY

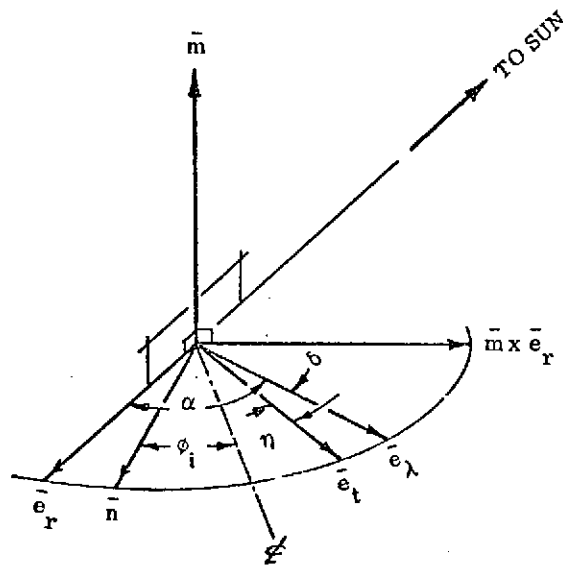


Fig. 2. Orientation geometry and nomenclature.

III. GENERALIZED RANK-PRESERVING SEARCH ALGORITHM

The following analysis was evolved by Samuel Pines and consists of a search algorithm designed to produce accelerated convergence in terms of significantly decreasing the number of operations per iteration.

In many problems involving the solution of a system of nonlinear equations, z , which are functions of a variable control vector, x , the required vector, \hat{x} , is arrived at by successively reducing the residual error vector to zero in a sequence of linear transformations. As the solution approaches the correct solution, the linear transformation approximation dominates, and the required solution is obtainable in an accelerated manner. In order to ensure that all states remain reachable during the iteration process, it is important that the rank of the linear transformation remains complete.

The method outlined in this section possesses the acceleration quality, makes no assumptions of symmetry in the desired transformation, is rank preserving and reduces the errors in the transformation to zero in a least square sense. The method applies to systems of nonlinear equations in which the number of equations is equal to the number of control variables.

In the analysis which follows, x is the control vector of dimension n , z is the nonlinear n vector output as a function of x , \hat{z}_D is the desired output n vector, y_i is the residual error vector, $z_i(x_i) - \hat{z}_D$, \hat{x} is the desired control vector whose output is $\hat{z}_D(\hat{x})$, A is the local linear ($n \times n$) transformation, H_i is the approximation to the inverse of the matrix A , and α is a positive scalar. Equation numbers referenced in this section pertain to this section only.

In the derivation of the search algorithm, we assume that in the neighborhood of the desired solution, \hat{x} , the problem has a linear representation in matrix vector form which is given by

$$\hat{z}_D(\hat{x}) = z_i(x_i) + A(z_i(x_i), x_i) \{\hat{x} - x_i\}.$$

The matrix, A , is assumed to be unavailable, or too cumbersome to compute. However, we assume that we have a numerical process by which we can readily compute the vector output, $z_i(x_i)$, for each given control vector, x_i . The final solution is given by

$$\hat{x} = x_i - A^{-1} y_i,$$

where

$$y_i = z_i(x_i) - \hat{z}_D(\hat{x}).$$

Let H_1 be an a priori, full rank, approximation to the desired A^{-1} matrix, and let x_1 and y_1 be the initial estimate of the control and the error in its output from the desired output, respectively. For any control, x_i , we have the improved control, x_{i+1} , given by

$$x_{i+1} = x_i - \alpha_i H_i y_i, \quad (3-1)$$

where α_i is a positive numerical scalar so chosen that the resulting residual in the output $y_{i+1}(x_{i+1})$, is smaller in magnitude than the magnitude of the previous, $y_i(x_i)$. The full linear step in $x_{i+1} - x_i$ corresponds to $\alpha_i = 1.0$. To obtain the next approximation in A^{-1} , we produce H_{i+1} with the following properties:

$$\{y_{i+1} - y_i\}^T H_{i+1}^T = \{x_{i+1} - x_i\}^T + \delta x^T,$$

$$H_{i+1}^T = H_i^T + \delta H_i^T.$$

These are the $n^2 + n$ equations in n^2 unknowns, and we will obtain a solution for H_{i+1} which minimizes the sum of the squares of the $n^2 + n$ elements of δx and δH_i .

Let

$$\Delta x_i = x_{i+1} - x_i,$$

$$\Delta y_i = y_{i+1} - y_i.$$

The least squares solution for H_{i+1} is given by

$$H_{i+1} = H_i - \frac{1}{1 + \Delta y^T \Delta y} \{H_i \Delta y_i - \Delta x_i\} \Delta y_i^T.$$

To investigate the rank of H_{i+1} , we note from Eq. (3-1) that

$$H_{i+1} = H_i \left(I - \frac{1}{1 + \Delta y^T \Delta y} \{ \Delta y_i - \alpha y_i \} \Delta y_i^T \right).$$

Thus rank $(H_{i+1}) = \text{rank}(H_i)$ provided the determinant

$$\det \left(I - \frac{1}{1 + \Delta y^T \Delta y} \{ \Delta y_i - \alpha y_i \} \Delta y_i^T \right) \neq 0. \quad (3-2)$$

The determinant will not vanish provided

$$\alpha \neq \frac{1}{\Delta y_i^T y_i}.$$

But, if for a positive α , $|y_{i+1}| < |y_i|$ we have

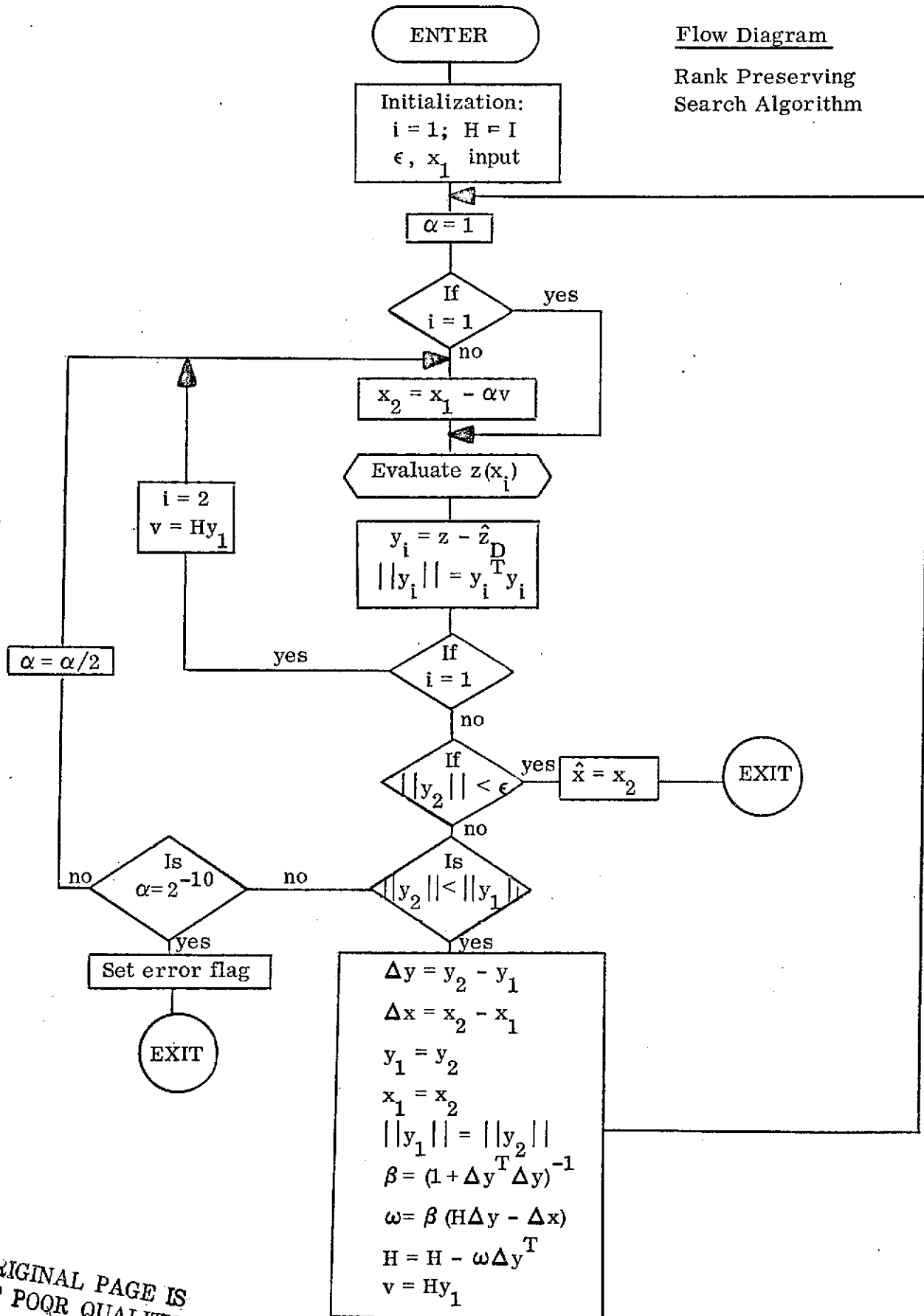
$$\alpha > 0 > y_{i+1}^T y_i - y_i^T y_i,$$

so that the rank preserving inequality of Eq. (3-2) is always satisfied for an acceptable correction step in the control.

The advantage of this iterator is that once a reasonable estimate of an initial H is available, no matrix inversions are required nor is there any necessity to generate, either through analytical equations or differential corrections, a matrix of partials of the dependent parameters with respect to the independent parameters. A limitation of the iterator is that the number of dependent and independent parameters must be equal. In any specific application, the most critical factor, in terms of overall efficiency, will be the algorithm for controlling the parameter α .

This search algorithm has been incorporated into a breadboard computer program using the identity matrix as an initial estimate of H and a simple control law for α , and its convergence ability has been demonstrated. The logical sequence of the experimental computer program is given in the flow chart presented on the following page. The full potential of this new search algorithm has yet to be explored.

Flow Diagram
Rank Preserving
Search Algorithm



ORIGINAL PAGE IS
OF POOR QUALITY

IV. TRAJECTORY OPTIMIZATION CONSIDERING THRUSTER THROTTLING

With SEP, the power generated by the solar arrays and input to the power conditioning units varies continuously with distance from the sun. The utilization of this varying power by the thruster subsystem will, to some extent, vary with the assumed design of the thruster subsystem. The model incorporated in the HILTOP program assumes constant efficiency and jet exhaust speed throughout a mission. Since hardware design considerations preclude these operating conditions, except possibly at non-optimal settings, it is desired to learn the effects on performance of simulating a more realistic thruster subsystem control policy. The formulation of such a simulation capability in the HILTOP program is presented in this section. Again, knowledge of the nomenclature and formulation of HILTOP as presented in [1] is assumed.

This analysis assumes that the thruster subsystem is comprised of a number of individual thrusters, each of which is characterized by a reference power p_t which represents a maximum allowable input power. The throttling ratio q is defined as the power input to the thruster subsystem divided by the total allowable power input to the n_t operating thrusters, i.e.,

$$q = \frac{p_{\text{ref}}^\gamma}{n_t p_t},$$

where p_{ref} is the reference power available to the power conditioning units at 1 AU from the sun and γ is the ratio of power at a distance r to power at 1 AU. This implies that all thrusters currently in use are operating at the same throttling ratio. The formulation employed is based on the assumption that individual thrusters are turned on or off as necessary to make optimum use of the power that is available and to satisfy any constraint on a minimum allowable throttling ratio q_m .

The variations in jet exhaust speed c and efficiency η are assumed to be specified functions of q . The precise form is not important here; we will simply write

PRECEDING PAGE BLANK NOT FILMED

$$c = c(q); \quad \eta = \eta(q),$$

with the boundary conditions

$$c_1 = c(1); \quad \eta_1 = \eta(1),$$

applying at $q=1$.

Employing the nomenclature of the HILTOP users' manual^[1], the formulation for the throttling capability is as follows. Define at each point along the trajectory the number of operating thrusters n_t as the smallest integer such that

$$n_t \geq \frac{p_{\text{ref}}^\gamma}{p_t}.$$

Then the throttling ratio of each operating thruster is defined

$$q = \frac{p_{\text{ref}}^\gamma}{n_t p_t}.$$

If, however, this value of q is less than the input q_m , it is necessary to decrement n_t by one, after which

$$n_t p_t < p_{\text{ref}}^\gamma,$$

and q is reset to unity. This results in the utilization of less power than is available to the power conditioning units, and it is assumed that this excess power is radiated off in space* with no penalty in performance. Then the thrust acceleration that the propulsion system is capable of generating at any instant may be written

$$a = \frac{2 n_t p_t q \eta}{m_o c \nu}.$$

For comparison, the thrust acceleration in the HILTOP formulation was written

$$a = \frac{a_o \gamma}{\nu}.$$

*Or the solar panels are tilted so that only the power required is produced.

The optimal switching of individual thrusters is determined from the maximum principal. The variational Hamiltonian is written

$$h_v = h_\sigma \left[a(\Lambda \cdot \bar{e}_t - \frac{\nu}{c} \lambda_\nu) + \lambda_\tau \right] - \frac{\mu}{r^3} \Lambda \cdot R - \dot{\Lambda} \cdot \dot{R}.$$

Defining the switch function σ as

$$\sigma = \sigma^* + \lambda_\tau / a,$$

where

$$\sigma^* = \Lambda \cdot \bar{e}_t - \nu \lambda_\nu / c,$$

it is seen that

$$h_\sigma = \begin{cases} 0 & \text{if } \sigma < 0 \\ 1 & \text{if } \sigma > 0 \end{cases}.$$

When $h_\sigma = 1$, optimal switching of individual thrusters is governed by choosing the number that maximizes $a\sigma^*$. If $\dot{\gamma} < 0$, clearly the choice is whether to continue using the current number of thrusters or to turn one off. Conversely, if $\dot{\gamma} > 0$, the question is whether another thruster should be turned on. Consider first the case where $\dot{\gamma} < 0$ in which one looks for the condition

$$\frac{n_t q \eta}{c} \left(\Lambda \cdot \bar{e}_t - \frac{\nu \lambda_\nu}{c} \right) = \frac{(n_t - 1)}{c_1} \left(\Lambda \cdot \bar{e}_t - \frac{\nu \lambda_\nu}{c_1} \right) \eta_1,$$

to be satisfied. When this occurs, n_t is decremented and the thrust acceleration is discontinuous although the Hamiltonian and all adjoint variables are continuous. After decrementing n_t , the condition,

$$n_t p_t < p_{\text{ref}} \gamma,$$

will exist for a finite period of time during which the power utilized is held constant, and the power differential $p_{\text{ref}} \gamma - n_t p_t$ is radiated into space. This condition is maintained until γ decreases to the point for which the inequality becomes an equality after which the thrusters are again throttled as necessary.

The case for $\dot{\gamma} > 0$ is basically the reverse of the above. The n_t thrusters are throttled up until $q = 1$ is reached. Thereafter constant power is utilized until the condition

$$\frac{n_t \eta_1}{c_1} \left(\Lambda \cdot \bar{e}_t - \frac{\nu \lambda \nu}{c_1} \right) = \frac{(n_t + 1) q_p \eta_p}{c_p} \left(\Lambda \cdot \bar{e}_t - \frac{\nu \lambda \nu}{c_p} \right)$$

is satisfied where

$$q_p = \frac{p_{\text{ref}} \gamma}{(n_t + 1) p_t},$$

and η_p and c_p are the efficiency and jet exhaust speed, respectively, evaluated for $q = q_p$.

The above conditions for optimally switching individual thrusters apply if, at the switch point, q for $\dot{\gamma} < 0$ or q_p for $\dot{\gamma} > 0$ exceeds q_m . If this is not the case, then the switch is made when the condition

$$q = q_m \quad \text{if } \dot{\gamma} < 0,$$

or

$$q_p = q_m \quad \text{if } \dot{\gamma} > 0,$$

is satisfied. When this occurs, the quantity $a \sigma^*$ is discontinuous, but the Hamiltonian remains continuous due to a corresponding jump in the primer derivative $\dot{\Lambda}$. Letting the superscripts - and + denote limiting conditions before and after the switch, respectively, the discontinuity in $\dot{\Lambda}$ may be written

$$\dot{\Lambda}^+ = \dot{\Lambda}^- + \frac{(a \sigma^*)^+ - (a \sigma^*)^-}{R \cdot R} R.$$

This equation applies also when the last thruster is switched on or off, at which time either a^+ or a^- is zero. Note that the decision to switch on or off individual thrusters must be made after every integration step, and if the decision is to switch, an iteration to the switch point is required prior to continuing integration.

Due to the dependence of c and η on q which, in turn, is a function of r , the second order differential equations for the primer vector become

$$\ddot{\Lambda} = \frac{2p_{\text{ref}} \eta \gamma'}{m_o \nu c r} \left[\sigma^* \left(1 - q \left(\frac{1}{\eta} \frac{d\eta}{dq} + \frac{1}{c} \frac{dc}{dq} \right) \right) - \frac{q \nu \lambda}{c^2} \frac{dc}{dq} \right] R$$

$$+ \frac{3\mu}{r^5} (\Lambda \cdot R) R - \frac{\mu}{r^3} \Lambda.$$

Furthermore, since c is strictly a function of q , there is no point in including c as a state variable. Therefore, the differential equation for λ_c may be eliminated.

V. INFINITESIMAL THRUST/COAST PHASES

In the performance of a typical mission study, one frequently desires to generate a sequence of optimal trajectories over a range of values of one or more independent parameters. A standard approach in such a study is to use the results of one converged case as initial guesses to the solution of the next case in the sequence. When employing a variational calculus program, such as HILTOP, in this situation, a convergence problem occasionally arises that deserves special attention. If, as one progresses through the sequence, a new thrust or coast phase appears in or disappears from the solutions, it is not uncommon to experience severe difficulty, or failure, in convergence near the transition solution. Although this problem will arise in only a very small percentage of cases, the analyst will find that such problems will consume the greatest proportion of his and the computer's time over the course of the data generation task. Consequently, the solution of this problem would yield a significant cost reduction in electric propulsion mission analysis. Unfortunately, no real progress has been made in solving this problem. The following paragraphs explain the behavior of HILTOP as the problem is encountered.

Consider, as an example, a sequence of cases in which the switch function passes through a positive minimum in the same general region of the several cases in the sequence. Suppose that, as one progresses through the sequence, the value of the switch function at the minimum decreases to the point that, on the next case of the sequence, one would predict that the minimum value will be negative. That is, on the next case one would predict a small coast phase in the vicinity of the minimum in the switch function.

In using HILTOP in a situation such as this, one should expect, at best, an increase in the number of iterations required for convergence and, at worst, failure to converge. The reason for this is that the behaviors of two neighboring trajectories, one with the coast phase and the other without, are different when subjected to the same perturbations in the independent parameters. Another way

of saying this is that the partial derivative matrix will not be continuous or smooth across the transition.

To understand the behavior of HILTOP when this situation arises, it is necessary to consider the characteristics of the iterator MINMX3. Given a vector ΔY of desired changes in the end conditions, the partial derivative matrix P , and two arbitrarily defined diagonal positive-definite weighting matrices W_x and W_y , the independent parameter correction vector ΔX is obtained by solving the following set of simultaneous equations.

$$(P^T W_y P + \lambda W_x) \Delta X = P^T W_y \Delta Y$$

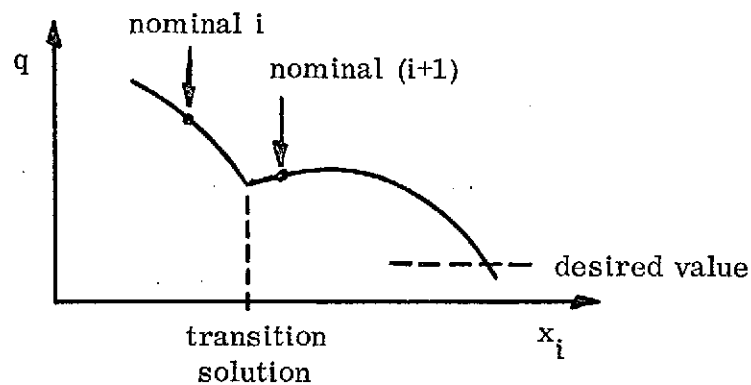
The scalar λ is termed the inhibitor and it controls the step size taken on a single iteration. Note that if $\lambda = 0$, the formula degenerates to the standard Newton-Raphson algorithm. Conversely, as λ approaches infinity, the correction ΔX approaches the null vector since the right hand side is finite. On each iteration MINMX3 automatically adjusts λ to control the step size on the next iteration. For this purpose, the scalar quantity

$$q = \Delta Y^T W_y \Delta Y,$$

which represents a weighted sum square of the residuals, is formed. The iterator is designed to require that no trial trajectory may be accepted as the next nominal unless the value of q for that trial is less than the value of q on the last nominal. Since one is guaranteed an improvement in q by setting λ to a sufficiently large value (i.e., by taking a sufficiently small step), the step size control algorithm consists simply of the logic required to successively increase λ until a value of q is achieved that is less than that of the nominal. Once this is accomplished, partial derivatives are produced for the new nominal and λ is reduced by a fixed factor in preparation for the next iteration.

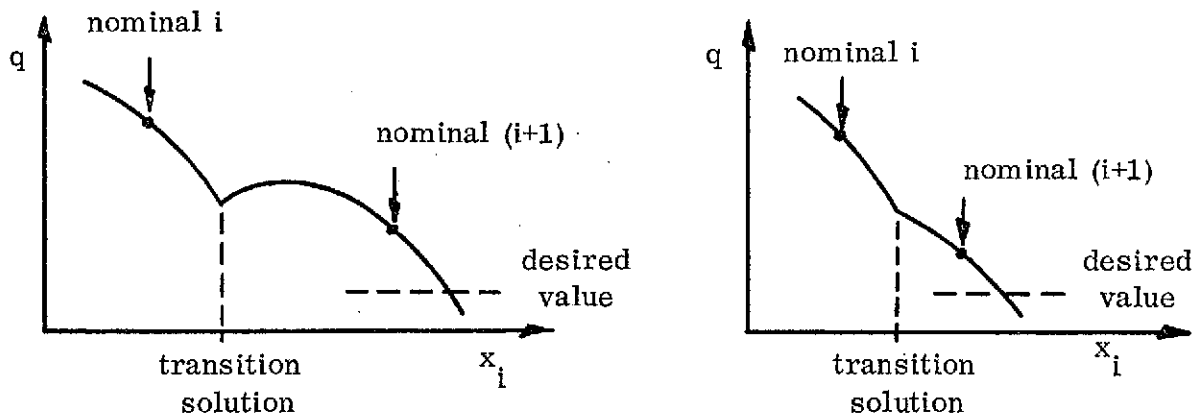
With the above algorithm in mind, consider once again the example hypothesized earlier. On the last case without the coast phase, a correction

vector ΔX is evaluated which normally will introduce the coast phase. Because the partials are incorrect for trial solutions with the coast phase, the scalar q will normally be larger than for the nominal. Consequently, λ is increased to reduce the step size. Typically, one of three situations will then develop. (1) The value of q on solutions with coast phases is always larger than the nominal. This results in the choice of nominal trajectories that are always on the same side of the transition, with successively smaller and smaller correction vectors resulting from larger and larger values of the inhibitor. Eventually, the correction vector is smaller than the least significant digits of the independent parameter vector and the iteration is terminated. (2) Nominals are selected on both sides of the transition; however, partial derivatives evaluated on both sides drive the solution toward the transition case where the switch function passes through a minimum with a value nearly zero. This condition terminates the iteration in the same manner as above. Conceptually in this case the problem is caused by the function q not being a smooth, convex function of the independent parameters. The situation in two dimensions may be depicted as shown in the following sketch. Note that locally the apparent correct



choice of the independent parameter x_i is in the direction of the transition solution.

(3) A step ΔX is taken which yields a new nominal with a small coast phase and which subsequently leads to the converged solution. In the context of the hypothetical two-dimensional case sketched above, either of the two situations depicted in the sketches below would lead to the desired result.



To this point, no satisfactory algorithm has been found which assures that the third condition above is established in an arbitrary situation. The following two steps have been taken and are employed routinely in the HILTOP: (1) the wasting of some CPU time is avoided by terminating a case after an input number of trajectories have been encountered in which the magnitude of the switch function at a stationary point is less than a specified tolerance, and (2) consistency in the partial derivative matrix is maintained by adjusting the perturbation step sizes as necessary to ensure the same number of switch points on the nominal and all perturbation trajectories.

VI. CURSORY TRAJECTORY ANALYSIS OF THE EXTRA-ECLIPTIC MISSION

Due to the recent interest in the extra-ecliptic mission as a possible engineering test flight for SEP, a cursory investigation of launch opportunities and performance requirements was undertaken for this mission. The basic mission considered terminated in a circular heliocentric orbit of nominally 1 AU radius with ecliptic inclination ranging from 45 to 60 degrees. The launch year chosen for the study is 1979; however, the solutions obtained repeat annually and are valid for any launch year.

Extra-ecliptic missions are noted for their requirement for relatively large geocentric declination of the hyperbolic launch asymptote. If one neglects the effects of declination on launch vehicle performance, the declination will vary from about 50 degrees to about 70 degrees, depending on the time of year of launch. The lower declinations occur for launches around the vernal equinox (negative declinations) and the autumnal equinox (positive declinations). In HILTOP, the launch vehicle performance is modelled as a function of the hyperbolic excess speed v_{∞} , the parking orbit inclination i if greater than the launch site latitude, and the geocentric declination δ of the asymptote if greater than the parking orbit inclination. The program permits any one of these three parameters to be fixed or optimized independently of the other two. Generally speaking, if i is allowed to be optimized the resulting value will nearly equal the declination. This is because the penalty in launch vehicle performance is much less for changing parking orbit inclination than for an equivalent non-coplanar injection maneuver from parking orbit. Certain launch vehicles are restricted to maximum parking orbit inclinations, however, due to range safety considerations. Such is the case for the Titan III E/Centaur launch vehicle which was specified for the study under discussion here. Consequently, the geocentric parking orbit inclination was limited to a maximum of 36 degrees, which was used in all cases generated. The other two parameters, v_{∞} and δ , were optimized to yield maximum final mass. This approach to the inclusion of the effects of large launch asymptote declinations results in a finite, non-zero angular offset of the initial thrust acceleration vector

from the launch asymptote. This offset is in the plane of the excess velocity and the polar axis of Earth and is in the direction of the North Pole for positive declinations and the South Pole for negative declinations. That is, the excess velocity always lies between the initial thrust acceleration (i.e., the initial primer vector) and the equatorial plane. This offset angle is denoted α .

Mission durations ranging from 1.5 to 3 years were to be investigated. Over such a broad range of flight times, it is essential that more than one class of missions be studied. A mission class for the extra-ecliptic mission may generally be categorized in terms of the number of burns. Typically one burn will occur around every nodal crossing such that, over an entire mission the number of burns n may be determined as a function of the number of revolutions r as follows:

$$n = 2r + 1 .$$

Previous studies for the 1 AU circular final orbit have yielded the result that the preferable class of solutions is that for which the trajectory remains in the vicinity of 1 AU throughout the mission. This is achieved by choosing the number of revolutions equal to the flight time t_f in years. For this reason mission classes of 4, 5, 6 and 7 burns were chosen for the flight times of 1.5, 2, 2.5 and 3 years, respectively.

In commencing the study, an attempt was made to optimize the launch date, along with several other parameters, for fixed flight time and final ecliptic inclination. Considerable difficulty in convergence was encountered, however, until the launch date was fixed. A sequence of solutions over a range of fixed launch dates then indicated that the final mass was very insensitive to the launch date, varying only a few hundredths of a kilogram over a launch date range of 2-3 weeks. The convergence problem was caused by the fact that the time transversality was not a monotonic function of launch date. This situation causes the iterator to "hang-up" at the local extremum in the transversality condition, leading to a singularity in the boundary value problem. By forcing the solution away from the singular point

to the locality of the true optimum, convergence to the optimum launch date can be achieved. But since the improvement in final mass was negligible the additional effort required to obtain the overall optimum was felt to be unwarranted. Consequently, the launch date for all cases generated in this study was fixed at April 21, 1979, which is about one month after the vernal equinox passage.

Numerical difficulty was also encountered as a result of an attempt to drive the final state to correspond to a circular orbit of exactly 1 AU. A ground rule of the study was that at distances below 1 AU, the arrays are to be tilted such that the power generated equals that developed at 1 AU. The simulation of this effect results in a discontinuity in slope of the power factor γ at the distance of 1 AU. The numerical problem arose as the solution neared convergence when neighboring trajectories would terminate on opposite sides of the 1 AU threshold. In effect, we were left with a problem not unlike that resulting from the infinitesimal thrust/coast phases discussed in the preceding section in which the partial derivative matrices differed on opposite sides of the threshold. The problem was alleviated by choosing a final circular orbit radius of 1.001 AU which is sufficiently far from the point of discontinuity to eliminate the convergence difficulty, yet near enough to the desired radius that the performance results are valid.

The other ground rules of the study were as follows:

- (1) a housekeeping power of 650 watts is to be provided;
- (2) total array power is 21 kw, leaving a reference power of 20.35 kw;
- (3) specific mass of the array is 15 kg/kw;
- (4) specific mass of the rest of the propulsion system is 15 kg/kw;
- (5) propellant tankage factor is 0.035;
- (6) total propulsion system efficiency is 0.63;
- (7) specific impulse is 3000 seconds.
- (8) optimize thrust direction, switch points, excess speed, geocentric declination, burn time and travel angle.

The results of the trajectory study are presented in the following table. The data are tabulated for the four flight times t_f as a function of the final ecliptic inclination i over the range of 45 to 60 degrees in increments of three degrees. The first several columns, including the initial adjoint variables λ_{x_0} , λ_{y_0} , λ_{z_0} , λ'_{x_0} , λ'_{y_0} and λ'_{z_0} , the reference thrust acceleration g , the hyperbolic excess speed v_∞ , and the geocentric asymptote declination δ , comprise the independent parameters of the boundary value problem. These parameters are necessary to reproduce the case with HILTOP. The remaining columns contain, in order, the initial thrust offset angle α , the change in ecliptic longitude over the mission $\Delta\lambda$, burn time t_b , initial spacecraft mass m_0 , final spacecraft mass m_f , maximum solar distance encountered r_{\max} , and minimum solar distance encountered r_{\min} .

EXTRA-ECLIPTIC MISSION PERFORMANCE STUDY

t_f (years)	l (deg)	λ_{x_0}	λ_{y_0}	λ_{z_0}	λ'_{x_0}	λ'_{y_0}	λ'_{z_0}	g (10^{-4} m/sec ²)	v_∞ (m/sec)	δ (deg)	α (deg)	$\Delta\lambda$ (deg)	t_b (days)	m_o (kg)	m_f (kg)	r_{max} (AU)	r_{min} (AU)
3	45	.0581	-.4030	-4.4916	.5860	.5305	-.3001	2.3278	4327.6	-37.137	-34.525	1118.1	831.81	3744.1	1621.3	1.0157	.8483
3	48	.0480	-.4032	-4.6367	.6241	.5625	-.3020	2.4267	4580.2	-37.362	-34.149	1116.6	830.69	3591.5	1472.8	1.0173	.8427
3	51	.0361	-.3949	-4.7406	.6522	.5850	-.3022	2.5249	4806.5	-37.578	-33.729	1114.8	828.22	3451.8	1340.5	1.0184	.8380
3	54	.0234	-.3800	-4.8100	.6715	.5991	-.3010	2.6218	5010.2	-37.782	-33.284	1112.7	824.78	3324.3	1222.9	1.0190	.8338
3	57	.0102	-.3600	-4.8493	.6830	.6059	-.2983	2.7171	5194.6	-37.972	-32.822	1110.6	820.62	3207.7	1117.4	1.0193	.8302
3	60	-.0035	-.3369	-4.8635	.6886	.6079	-.2953	2.8106	5362.3	-38.150	-32.363	1108.3	815.93	3100.9	1023.2	1.0193	.8270
2.5	45	.0015	-.3713	-5.1923	.7087	.6353	-.3264	2.6665	5099.6	-37.854	-32.787	939.1	714.95	3268.5	1447.4	1.0190	.8296
2.5	48	-.0185	-.3445	-5.2929	.7284	.6490	-.3278	2.7906	5328.6	-38.092	-32.181	937.2	712.13	3123.2	1309.8	1.0191	.8252
2.5	51	-.0384	-.3133	-5.3571	.7391	.6547	-.3276	2.9122	5532.8	-38.308	-31.585	935.0	708.66	2992.8	1188.4	1.0186	.8215
2.5	54	-.0611	-.2834	-5.3924	.7469	.6620	-.3316	3.0315	5716.7	-38.508	-31.040	933.0	704.77	2875.0	1081.0	1.0189	.8181
2.5	57	-.0863	-.2499	-5.4013	.7497	.6663	-.3381	3.1489	5884.0	-38.689	-30.491	931.0	700.54	2767.8	985.6	1.0200	.8146
2.5	60	-.1150	-.2061	-5.3857	.7434	.6625	-.3450	3.2647	6038.2	-38.884	-29.864	928.8	696.04	2669.6	900.6	1.0230	.8108
2	45	-.0837	-.3036	-5.9621	.8182	.7355	-.3506	3.1613	5899.3	-38.736	-30.714	758.5	589.13	2756.9	1252.2	1.0133	.8168
2	48	-.1200	-.2739	-6.0371	.8449	.7650	-.3766	3.3206	6105.2	-38.977	-30.141	757.2	585.82	2624.7	1128.9	1.0152	.8137
2	51	-.1613	-.2279	-6.0708	.8511	.7791	-.4022	3.4756	6289.1	-39.176	-29.472	755.9	582.55	2507.7	1021.0	1.0170	.8100
2	54	-.1991	-.1874	-6.0782	.8580	.7930	-.4269	3.6275	6454.9	-39.357	-28.882	754.3	578.90	2402.6	935.9	1.0192	.8071
2	57	-.2355	-.1462	-6.0592	.8591	.8020	-.4496	3.7758	6605.1	-39.515	-28.311	752.5	575.12	2308.3	842.2	1.0216	.8045
2	60	-.2708	-.1040	-6.0165	.8543	.8061	-.4700	3.9206	6742.1	-39.651	-27.750	750.6	571.23	2223.0	767.9	1.0244	.8019
1.5	45	-.3773	.0309	-6.8950	.8872	.8451	-.5402	3.9719	6797.2	-39.551	-26.548	581.2	455.84	2194.3	1034.1	1.0249	.7936
1.5	48	-.4584	.1277	-6.9330	.8748	.8559	-.5891	4.1913	6986.9	-39.684	-25.539	579.8	453.17	2079.4	928.0	1.0306	.7880
1.5	51	-.5434	.2334	-6.9331	.8478	.8575	-.6349	4.4066	7158.2	-39.769	-24.486	578.1	450.45	1977.8	836.0	1.0376	.7816
1.5	54	-.6320	.3482	-6.8972	.8070	.8502	-.6782	4.6178	7314.3	-39.807	-23.376	576.3	447.71	1877.4	755.7	1.0463	.7741
1.5	57	-.7258	.4745	-6.8286	.7514	.8337	-.7192	4.8257	7458.4	-39.794	-22.171	574.3	444.96	1806.1	685.5	1.0568	.7651
1.5	60	-.8267	.6154	-6.7294	.6799	.8078	-.7585	5.0313	7593.1	-39.727	-20.832	572.1	442.25	1732.3	623.7	1.0698	.7541

ORIGINAL PAGE
OF POOR QUALITY

VII. REFERENCES

- [1] F. I. Mann and J. L. Horsewood, "Program Manual for HILTOP, A Heliocentric Interplanetary Low Thrust Trajectory Optimization Program," AMA, Inc. Report No. 74-34, December, 1974.
- [2] J. L. Horsewood, "Program Manual for ASTOP, An Arbitrary Space Trajectory Optimization Program," AMA, Inc. Report No. 74-33, December, 1974.

PRECEDING PAGE BLANK NOT FILMED